

Polymeric Hydrogels Obtained Using a Redox Initiator: Application in Cu(II) Ions Removal from Aqueous Solutions

José Luis Morán-Quiroz,¹ Eulogio Orozco-Guareño,¹ Ricardo Manríquez,² Gregorio G. Carbajal-Arízaga,¹ Wencel de la Cruz,³ Sergio Gomez-Salazar⁴

¹Departamento de Química, Centro Universitario de Ciencias Exactas e Ingenierías, Universidad de Guadalajara, Blvd. Marcelino García Barragán 1451. Guadalajara, Jalisco, México

²Departamento de Madera, Celulosa y Papel, Centro Universitario de Ciencias Exactas e Ingenierías, Universidad de Guadalajara, Km 15.5, Carretera Guadalajara-Nogales, Guadalajara, Jalisco 45020, México

³Centro de Nanociencias y Nanotecnología, Universidad Nacional Autónoma de México, Km 107 Carretera Tijuana-Ensenada, Ensenada, Baja California 22830, México

⁴Departamento de Ingeniería Química, Centro Universitario de Ciencias Exactas e Ingenierías, Universidad de Guadalajara, Blvd. Marcelino García Barragán 1451. Guadalajara, Jalisco, México

Correspondence to: S. Gomez-Salazar (E-mail: sergio.gomez@cucei.udg.mx)

ABSTRACT: Poly(acrylic acid-co-acrylamide) hydrogels were prepared via free-radical solution polymerization, crosslinked with ethylene-glycol-dimethacrylate, potassium persulfate/ammonium bisulfite as the initiator, and applied in the removal of Cu(II) ions from aqueous solutions. Molar ratios of acrylamide/acrylic acid moieties and the amount of crosslinking agent were varied to determine the swelling capacities of hydrogels and maximum metal uptake. Polymerization kinetics was investigated by ¹H-NMR. Hydrogel physicochemical properties were characterized by nitrogen sorption measurements, elemental analysis, FTIR, and X-ray photoelectron spectroscopy (XPS). Swelling results indicated that hydrogels were swollen up to 27,500%. Hydrogels showed equilibrium Cu(II) adsorption capacities of 211.7 mg g⁻¹ and fast kinetics (~20 min). Langmuir isotherm fitted adsorption equilibrium data. FTIR and XPS results helped in elucidating the presence of monodentate copper complex on the surface of hydrogels. A simple synthesis route of hydrogels using the redox initiator suggests the potential application in the removal of toxic metals from aqueous streams. © 2013 Wiley Periodicals, Inc. *J. Appl. Polym. Sci.* **2014**, *131*, 39933.

KEYWORDS: adsorption; copolymers; hydrophilic polymers

Received 26 April 2013; accepted 3 September 2013

DOI: 10.1002/app.39933

INTRODUCTION

Pollution problems are becoming so diverse and have increased in magnitude as much as the modern society is becoming more aware of the risks the pollutants pose to both human health and environment. One of these problems is the water pollution by heavy metals, caused in part by an increase in the number of wastewater discharges from many types of industrial activities, including chemical, metallurgic, paper, food, and electronics.¹ In some developing countries, these wastewaters receive little or null treatment and are discharged to the environment containing large amounts of metal ions such as mercury, chromium, lead, nickel, and copper.^{2,3} The concentrations of these ions are almost always above the permitted limits established by the regulations.³⁻⁷ Reduction of metal ion concentrations to comply with regulations is an industrial challenge and it has received considerable attention due to the high degree of toxicity of

these ions.^{8,9} For example, the toxic effects of Cu(II) ions to human health include gastrointestinal disturbances, such as nausea, abdominal pain, diarrhea, and vomit, and can appear if water concentrations of this metal exceed 6.0 mg L⁻¹.⁵ Because of these reasons, the maximum Cu(II) concentration in drinking water has been set to 2.0 and 1.3 mg L⁻¹ by the World Health Organization (WHO) and the United States Environmental Protection Agency (USEPA), respectively.^{4,5}

Several techniques have been used to reduce/eliminate heavy metal concentrations from industrial wastewaters, and these include precipitation,¹⁰ inverse osmosis,¹¹ electrodeposition,¹² and evaporation,¹³ among others.¹⁴⁻¹⁶ However, these techniques present several limitations. For instance, precipitation of the metal ions by using hydroxides or carbonates can reduce some metals to the parts-per-million level.¹⁷⁻¹⁹ This method fails in the presence of solubilizing agents like ammonia or cyanide that often

coordinate to the metal ion to form stable soluble complexes and prevent further metal precipitation.²⁰ During evaporation of wastewaters containing heavy metals, noxious gases such as sulfides can be produced.¹³ Reverse osmosis utilizes a semipermeable membrane to filter dissolved salts from water under pressures exceeding the osmotic pressure of the salts in solution. This process is limited by the capacity of the membrane to support long-term pressures and to withstand extreme pH.²¹ Since the preceding techniques have had limited success and efficiency in removing metal ions from aqueous streams, exists the need for alternate methods to remove these metal ions.

Polymeric hydrogels have demonstrated to have high capacities of Cu(II) uptake, since they can interact with the functional groups present along the hydrogel polymeric network.^{8,14–16,22–24} The metal uptake mechanism by hydrogels has been related to their high water permeability and to the presence of small solutes such as heavy metal ions. Specifically, hydrogels composed of acrylic monomers like acrylic acid (AA) and acrylamide (AM) have demonstrated to be good adsorbents towards heavy metals and some other multiple applications that are still under investigation.^{22–27} For instance, Xiao-Jie et al. synthesized an acrylic hydrogel like-adsorbent material that exhibited good ion recognition for Pb²⁺.²⁸ Hyun Jang et al.²⁹ obtained acrylic composite hydrogels for Pb²⁺ removal from aqueous solutions. For these materials, the removal mechanism was highly dependent on the solution pH. Ufuk Yildiz et al.,²⁷ synthesized nonionic hydrogels by radical homopolymerization of *N*-vinyl-2-pyrrolidone (VP) and by radical copolymerization of VP with methylacrylate (MA) as binding materials for Cu²⁺, Cd²⁺, Ni²⁺, and Zn²⁺, obtaining Cu²⁺ binding capacities of 60–110 mg Cu/g hydrogel at pH values of 2–8 in the case of the copolymer P(VP-*co*-MA). Consequently, the design of hydrogels with improved metal uptake capacities has to be based on the selection of functional groups, such as carboxylic, amide, etc, which are known to be good chelating sites to bind metal cations, as well as the type of both initiator and crosslinking agent.

In view of our interest in industrial applications of adsorptive hydrogels that can be obtained under mild reaction conditions, a simple synthesis route to prepare acrylic acid/acrylamide hydrogels, is presented here. The aim of this work was to synthesize and characterize acrylic acid/acrylamide-based polymeric hydrogels using a chemical initiator and different amounts of crosslinking agent expecting to obtain high ligand densities, improved metal ion uptake capacities, fast kinetics, and easily swollen structures to facilitate the entrance of metal ions to chelating sites. The Cu(II) uptake capacity of the hydrogels was compared with other polymeric materials including some biomaterials used for similar applications. The polymerization reaction evolution of hydrogels was studied *in situ* by using ¹H-NMR. The synthesized hydrogels were characterized by Elemental Analysis, N₂ adsorption measurements, FTIR, and X-ray photoelectron spectroscopy (XPS). The effect of monomer ratios used, solution pH, and metal concentrations on the extent of metal uptake by hydrogels were also investigated.

EXPERIMENTAL

Materials

Acrylic acid (AA, 99%), acrylamide (AM, 99%), and ethylene-glycol-dimethacrylate (EGDMA, 98%), as the crosslinking agent

were used as received (Sigma-Aldrich). Potassium persulfate (98%, Caledon) and ammonium bisulfite (98%, Fermont) were used as initiators. CuSO₄·5H₂O at 98% (Sigma-Aldrich) was used for the metal uptake experiments. Calibration curves and metal uptake experiments were performed with certified standard copper solutions of 1000 mg L⁻¹ (Sigma-Aldrich) and deionized water with 18 MΩm of resistivity.

Synthesis of Hydrogels

Polymerization by free-radical in solution was employed to synthesize poly(acrylic acid-*co*-acrylamide) hydrogels. In a typical experiment, (AA : AM weight ratio = 50 : 50, equivalent to a AA : AM molar ratio = 1 : 1), 27.7 g of AM (0.39 mol) was dissolved in 55 mL of water and 26.94 mL of AA (equivalent to 0.39 mol) was added to this mixture with a corresponding amount of EGDMA (0.55 g for 1 % wt). The resulting solution was fed into a 0.5 L rectangular reactor and the pH was adjusted to 7 with a 0.2M KOH solution. This mixture was stirred for 5 min and left to rest at 268 K for 24 h to control monomers side reactions in the redox polymerization process.^{30–33} Then, 3 mL of potassium persulfate (0.148M) solution and ammonium bisulfite (0.124M NH₄HSO₃) were added to the mixture and heated to 318 K for 2 h using a controlled temperature bath (LAUDA model E100). The resulting rectangular plate was dried at 333 K for at least 72 h. The dried hydrogels (xerogels) were thoroughly washed for 72 h with deionized water to eliminate monomer and KOH residues. Hydrogel samples were identified according to the monomer ratios employed, as follows: samples from group A corresponded to an AA : AM molar ratio of 1.2 : 1.0, samples from group B to an AA : AM molar ratio of 1.0 : 1.0 and samples from group C to an AA : AM molar ratio of 1.0 : 1.2. All samples in the three groups used 1, 4, 8, and 16 % wt of EGDMA. Thus, sample A1 corresponded to a hydrogel with an AA : AM molar ratio of 1.2 : 1.0 and 1 % wt of EGDMA; sample A4 corresponded to the same AA : AM molar ratio but with a 4 % wt of EGDMA, and so on. Same identification procedure was applied to samples in groups B and C.

Swelling Measurements

Swelling capacity of the hydrogels was evaluated through gravimetric measurements. Cylindrical-shaped xerogels (ca. 0.7 ID and 3-mm thick) were dried at 313 K and immersed in 500 mL of doubly distilled water at different times. The weight gained due to water absorption was registered; the swelling amount of hydrogels *S* reported as percentage and as a function of the immersion time was calculated by the following equation^{14,16,22–29}:

$$S(\%) = \left(\frac{W_s - W_d}{W_d} \right) \times 100 \quad (1)$$

where w_d and w_s represent the weights of dry and swollen hydrogels, respectively.

¹H-NMR Experiment

The progress of polymerization reaction was monitored by ¹H-NMR on sample A1, since this sample was the one that removed the highest amount of Cu(II). The measurements were made by placing into the NMR tubes, about 0.7 mL of a neutralized solution of monomers AA (0.82 g) and AM (0.27 g), EGDMA (0.022 g), and 1.1 mL of D₂O. Polymerization was

initiated by means of potassium persulfate and ammonium bisulfite. $^1\text{H-NMR}$ spectra of this sample were recorded *in situ* at different time intervals (0–90 min) before gelation occurred, using a 200 MHz spectrometer broadband Varian Gemini 2000. All spectra were taken at the proton frequency of 199.97 MHz and at 313 K.

Maximum Cu(II) Uptake and Adsorption Equilibrium Experiments

To determine the maximum Cu(II) uptake of hydrogels, an experiment was conducted on samples A1, A16, C1, and C16 by contacting 0.15 g of sample with 25 mL of a $1863 \pm 30 \text{ mg L}^{-1}$ copper initial solution at $\text{pH}_f = 4.4$, at 298 K and agitated for 1 h. Suspensions were filtered and the final solution analyzed for copper concentrations using atomic absorption spectrometry. The amount of copper adsorbed onto the xerogels q (mg g^{-1}), expressed on a xerogel mass basis, was calculated by a mass balance between the initial and final solutions and expressed by:

$$q = \left(\frac{C_o - C_f}{m} \right) V \quad (2)$$

where C_o and C_f represent the copper ion concentrations in the initial and final solutions (mg L^{-1}), respectively, V is the volume of contacting solution (L) containing the metal ions which remained constant between initial and final solutions, and m is the weight of the xerogel (g).

Equilibrium adsorption measurements were conducted in the batch mode on sample A1 to determine the maximum Cu(II) uptake in the pH range 3.0–5.0 to cover the range at which many industrial wastewaters are disposed.^{21,34,35} Previous to these measurements, hydrogel samples were rasped, ground, sieved (mesh no. 40) using ASTM II specifications for sieve trays (1.19–0.21 mm), swollen to maximum, and dried at 312 K for 72 h until constant weight. Samples obtained from this process are called xerogel. Several initial solutions with varying metal concentrations ($100\text{--}2000 \text{ mg L}^{-1}$) and fixed pH were prepared by dilution from a $2000 \pm 4.5 \text{ mg L}^{-1} \text{ CuSO}_4 \cdot 5\text{H}_2\text{O}$ stock solution. Xerogel amounts of 0.15 g were contacted with 25 cm^3 of initial solution for 1 h (which was the time when the amount of metal adsorbed remained unchanged) in an Environ-Shaker Model 3597 water bath at 298 K. Suspensions were filtered, the pH of initial and final solutions was measured with a Hanna Instruments model HI 98128 pH meter. Total copper concentrations in the solutions were analyzed using a Varian SpectraAA 220 atomic absorption spectrometer (Victoria, Australia). The amount of copper uptake per unit mass of hydrogel was determined by eq. (2). Triplicate measurements were conducted and averaged values are reported.

Kinetics of Copper Uptake by Xerogels

To investigate the effect of both monomer ratio and crosslinking agent on the Cu(II) uptake rate, kinetic experiments were conducted in a batch reactor on four samples (A1, A16, B1, and B16) at 298 K by using 20 cm^3 of a $300 \pm 1.5 \text{ mg L}^{-1}$ copper solution at initial pH 3. A sample of 0.1 g of xerogel (125–180 μm , and previously treated as described in the adsorption equilibrium measurements) was introduced into a 250 cm^3 reactor

at time 0; solution samples were taken at different times and filtered prior to the analysis of copper concentrations by atomic absorption spectrometry. The amount of copper uptake per unit mass of hydrogel was determined by eq. (2).

Elemental Analysis and N_2 Adsorption Measurements

The theoretical metal uptake capacity of the hydrogels was determined by elemental analysis of C, H, N on samples A1, A16, B1 y B16, with an EA 1108 Fisons Instrument model EA1108 CHNS. Nitrogen adsorption isotherms were obtained at 77 K on a Micromeritics Model ASAP 2020 (Norcross, GA). The samples (0.5 g) were heated at 353 K for 12 h under vacuum to remove all adsorbed species from the surfaces of xerogels. The BET surface area was calculated using adsorption data in the relative pressure range of 0.15–0.26 included in the validity domain of the BET equation.

FTIR Analysis

Vibrational behavior of the xerogel samples on Cu-free samples (A1 and A16) and samples saturated with copper (A1-Cu and A16-Cu), was studied by FTIR spectroscopy with a Perkin Elmer Spectrum One spectrophotometer using the potassium bromide disk technique. The IR spectra were the averages of 150 scans with a resolution of 4 cm^{-1} within a frequency range of $450\text{--}4000 \text{ cm}^{-1}$ at 298 K.

XPS Measurements

The synthesized xerogels were analyzed by XPS to determine the chemical states of the surface functional groups and to elucidate the nature of the surface copper complex formed. Measurements were performed with a RIBER XPS spectrometer. The base pressure in the analyzer was less than $4 \times 10^{-7} \text{ Pa}$. XPS spectra were taken using a dual-anode (Mg and Al) X-ray source, operating the Mg anode at 300 W (15 kV and 20 mA). Before the measurements, samples were conditioned for 2 h at 373 K. High-resolution scans were performed over the range 800–1000 eV (Cu 2p spectrum) with the pass energy adjusted to 50 eV. Survey scans for Cu 2p, N 1s, C1s, and O1s core-level spectra were taken on Cu-free samples (A1) and on samples saturated with copper (A1-Cu). After baseline subtraction, curve fitting was performed using the nonlinear least squares algorithm and assuming a Gaussian variable-proportion peak shape. The positions of deconvoluted peaks were determined according to reports from the literature and empirically derived values.

RESULTS AND DISCUSSION

$^1\text{H-NMR}$ Analysis

The polymerization reaction progress was monitored by $^1\text{H-NMR}$ measurements at different reaction times ($t = 0\text{--}90 \text{ min}$). Figure 1 shows the results of the AA/AM copolymerization processes using a mixture of potassium persulfate and ammonium bisulfite as initiator. As it can be observed, the initial spectrum ($t = 0$) shows two groups of multiplets due to the mixture of several spin couplings among vicinal vinyl hydrogens (α and β) of the AA and AM monomers centered at 5.5 and 5.9 ppm, respectively. Moreover, the most intense signal at 4.7 ppm corresponds typically to the solvent (DOH), and some weak signals between 1.0 and 4.5 ppm can be attributed to the crosslinking agent. In general, the polymerization carried out with redox initiators (like potassium

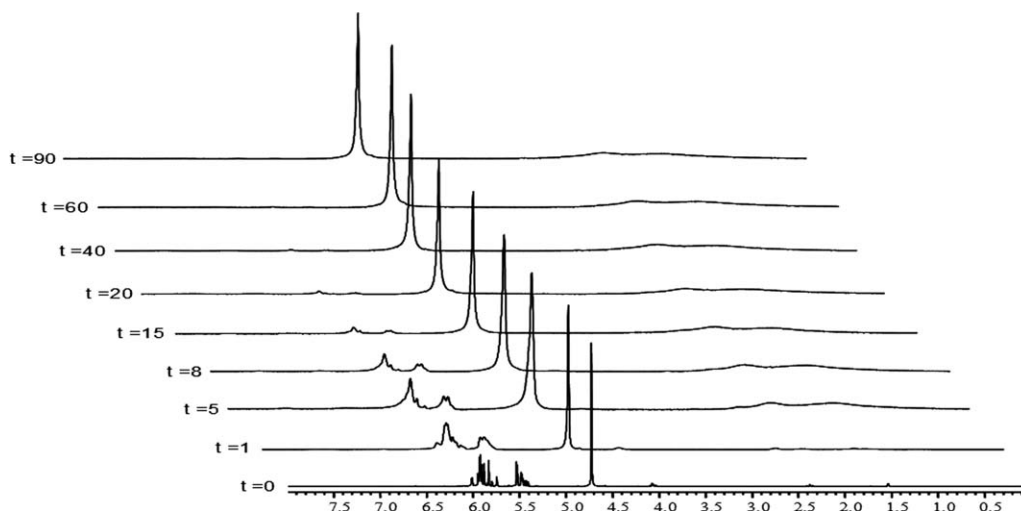


Figure 1. Polymerization reaction progress ($t = 0$ – 90 min) for sample A1 monitored by $^1\text{H-NMR}$ at 40°C .

persulfate and ammonium bisulfite) shows shorter polymerization times compared to the ones when the acrylic/acrylamide copolymer was obtained using photocatalysts.²² These results make the synthesis route used in this work more attractive to prepare polymeric hydrogels due to an ease of implementation and the use of room conditions. On the other hand, the $^1\text{H-NMR}$ spectra of Figure 1 shows that the polymerization progress can be appreciated clearly by the broadening of the vinyl hydrogen signals ($\delta = 5.5$ and 5.9 ppm) after 1 min (see spectrum at $t = 1$) and is almost complete after 20 min ($t = 20$) when the vinyl signals due to the AA/AM monomers are almost absent. Furthermore, the broad and weak signal intensity between 1.5 and 3.5 ppm confirms the formation of the AA/AM copolymer backbone as well as its poor solubility in the D_2O medium. Also, as a consequence of this polymerization process, the line width of the solvent signal (DOH) at 4.7 ppm became broader due to the anisotropic effect. This effect is caused by the different orientation of the water molecules due to organization of the chains in the polymer. The broadening of the DOH signal can reveal how the polymerization is taking place. In a previous work,²² the anisotropic effect was more noticeable because the DOH signal in the $^1\text{H-NMR}$ spectra became broader than the polymer shown in the present work. Based on this comparison, it can be postulated that the polymerization with photoinitiator could trigger the formation of several intermediate free-radical species attributed to a less organized polymer matrix³⁶ in comparison with the polymer catalyzed by our chemical redox initiator.

Swelling Properties of Hydrogels

The hydrophilicity property of the hydrogels was evaluated through the swelling experiments. The degree of swelling is used here to take advantage of the polymer chain opening to provide an easy access to the Cu(II) ions to the active sites. Figure 2 shows the results of swelling measurements for the three sets of hydrogel samples synthesized. It can be observed that, in general, the sets of curves corresponding to 1% EGDMA reached swellings of about 25,000% (samples B1 and C1) and 27,500% (sample A1). It is evident from the three plots

of this figure that swelling decreases as crosslinking agent amount increases. This trend is less evident for samples of group A (which contain an excess of AA), since swelling reached about 24,600% for sample A16. In the case of samples of group B (equimolar monomer ratio), the crosslinking agent causes a swelling decrease from 25,000% (1% EGDMA) to 17,000% (16% EGDMA). In the case of samples of group C (containing an excess of AM), swelling decreases to about 12,000% even with only 4% of crosslinking agent. This behavior has been attributed to a lower affinity of AM for water molecules compared to the one of AA.²² The polymeric chains of AA/AM hydrogels contain pendant carboxyl and amide functional groups, and depending on the medium (acid or basic), they can show protonated or deprotonated moieties (ionic form) as well. These groups are polar in nature and they confer the hydrophilic property to the hydrogels^{36,37} and interactions are promoted between these functional groups and water molecules through hydrogen bonds. The results obtained from the swelling measurements on our synthesized hydrogels, suggest strong interactions between water molecules and AA, and they agree with reports from literature.^{36–40} On the other hand, the crosslinking degree of hydrogels has a significant impact on the amount of water uptake by these materials by decreasing the swelling capacity due to structural restrictions in the polymer chain arrangement. As it was expected, the higher the crosslinking degree obtained the shorter the distances between the crosslinked points along the hydrogel chains.²³ In summary, the use of a chemical initiator of the polymerization reaction in this work appears more attractive for metal ion removal applications when compared to other types of initiators such as photoinitiators and UV light previously reported²² due to the mild reaction conditions of synthesis used in our work and improved metal uptake.

Kinetic Measurements

The kinetic results of copper adsorption onto hydrogel samples with two monomer ratios and varying amounts of crosslinking agent (A1, A16 and B1, B16) are shown in Figure 3. From these

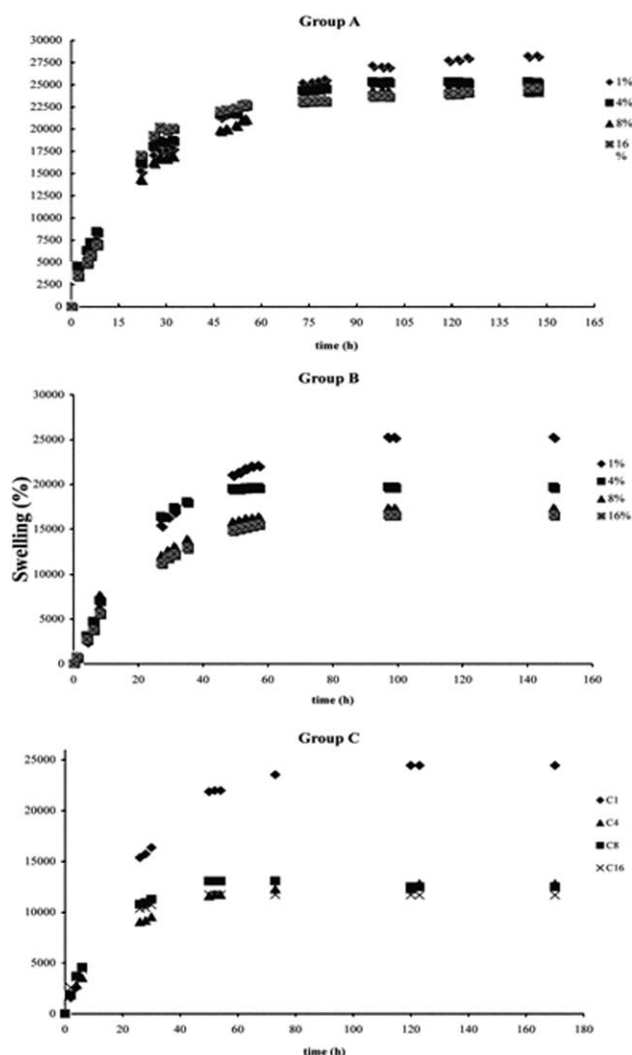


Figure 2. Swelling kinetics of hydrogels synthesized using different AA/AM ratios, a mixture of potassium persulfate and ammonium bisulfite as initiator, and several amounts of crosslinking agent (EGDM): (a) Samples from group A (AA : AM = 75 : 25), (b) samples from group B (AA : AM = 25 : 75), and (c) samples from group C (AA : AM = 50 : 50). (See text for group identification).

curves, some points can be addressed: (a) the determining factor in the sorption process is directly related to the composition ratio of AA/AM in the hydrogels and not to the copper ions nature. According to this, the relation between copper uptake and the nature of the AA/AM hydrogel is mainly driven by the reactivity of the COOH groups of AA, and to a lesser extent to the CONH₂ groups of AM, to undergo replacement reactions with the copper ions. (b) For the copper concentration examined, near equilibrium is attained in about 20 min for all samples. This result is important if the hydrogels are going to be used in the removal of metal ions from industrial streams. For all samples, attaining equilibrium at these times reflects the presence of minimal mass-transfer resistances. (c) The sharp decreasing trends in copper concentration in the interaction times are due to a lower crosslinking degree in samples A1 and A16 (higher interchain space).

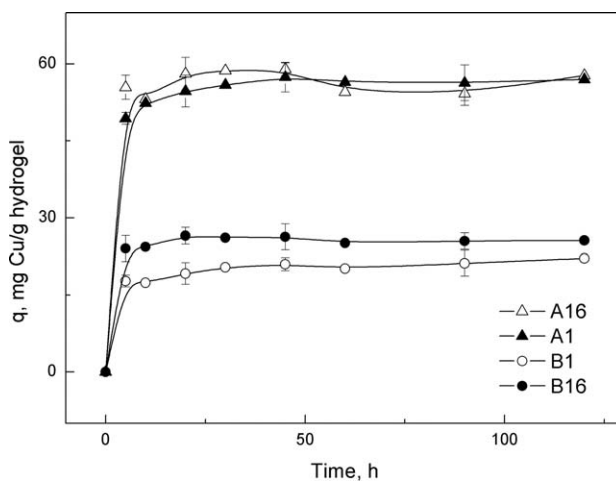


Figure 3. Adsorption kinetics of copper on four hydrogel samples using 20 cm³ of a 300 ± 1.2 mg L⁻¹ copper solution at pH 2 and 0.1 g of hydrogel (125–180 μm) at 298 K. Continuous lines are for visual guidance only.

Maximum Cu(II) Uptake and Adsorption Equilibrium Results

The maximum copper uptake is shown in Figure 4 for samples of hydrogels groups A and C. The maximum copper uptake observed of hydrogel sample A1 was 217.7 mg Cu/g hydrogel (or 3.33 mmol/g hydrogel). The hydrogels were regenerated with 50 cm³ of a 1.0M HCl solution with ~91% of the copper recovered. On the other hand, the sorption capacities of copper increased with an increase in the equilibrium metal concentration in solution, as it is evident from Figure 5. Moreover, the effect of solution pH on copper uptake is significant, where a higher copper uptake is observed at higher pH. This is due to a competition effect between the copper ions and protons from solution for the active sites on the surface of hydrogel and the sites located between the polymeric chains of hydrogel (mainly OH groups from the carboxylic acid). The interaction between the OH groups and copper ions is supported from the FTIR results. These results are in agreement with reports of research conducted on hydrogels for similar cations removal.¹⁶ It has been reported that hydrogels with swelling greater than 5000%,

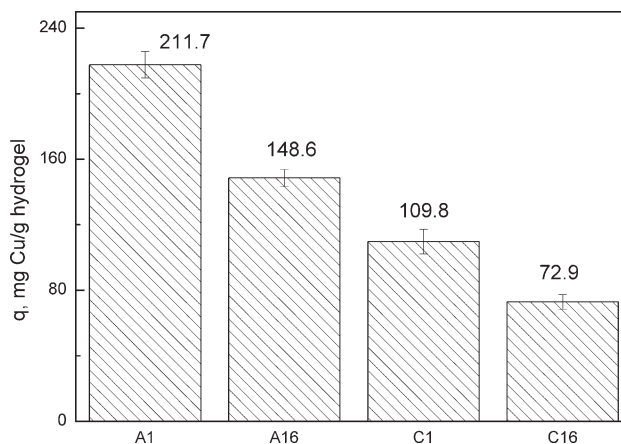


Figure 4. Maximum Cu(II) uptake on hydrogel samples A1, A16, C1, and C16. Experimental conditions: [Cu(II)]₀ = 1863 ± 30 ppm, pH_f = 4.4, T = 298 K, m = 0.15 g xerogel, V = 25 cm³, contact time = 1 h.

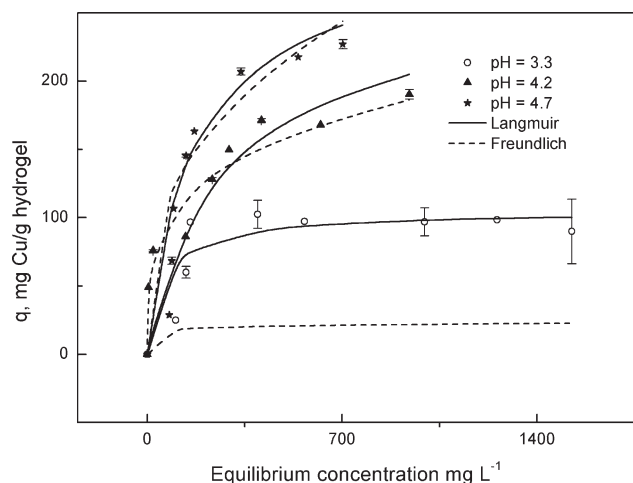


Figure 5. Adsorption isotherms for copper uptake by hydrogel sample A1 at three different solution pH values and fittings to Langmuir and Freundlich adsorption isotherms. Experimental conditions: solution volume = 25 cm³; hydrogel weight = 0.15 g; $T = 298$ K.

have polymer chains open and functional groups exposed, creating active sites with more possibility of interacting with the heavy metal ions.^{8–10,15,16,22} A study is in progress to investigate if there is a correlation between the amount of metal uptake and the degree of swelling of hydrogel.

To obtain a quantitative understanding of the adsorption phenomena of Cu ions on the synthesized hydrogels, Langmuir and Freundlich isotherms have been used to model the sorption process. The Langmuir isotherm assumes monolayer coverage of the adsorbate over homogeneous surface and equal sorption activation energy for the sorption of each molecule onto the

surface, while the Freundlich isotherm is derived by assuming a heterogeneous surface with a nonuniform distribution of heat of adsorption over the surface and can express multilayer sorption. The Langmuir and Freundlich isotherms may be expressed respectively as:

$$q = K q_{\max} C / (1 + KC) \quad (3)$$

$$q = aC^{1/n} \quad (4)$$

where q_{\max} is the maximum amount of copper adsorbed (mg g^{-1}), K is the sorption equilibrium constant (L mg^{-1}), C is the equilibrium concentration of the copper ions in the solution (mg L^{-1}), a is a constant representing the sorption capacity ($\text{mg}^{1-1/n} \text{L}^{1/n} \text{g}^{-1}$), and n is a constant depicting the sorption intensity. Figure 5 shows the sorption isotherms of copper ions on sample A1, since this sample showed the highest copper uptake; the Langmuir and Freundlich regressed constants are given in Table I. The regressed values of model parameters indicate that the proposed Langmuir model can predict the copper adsorption phenomena satisfactorily at pH 4.20 and 4.70. Overall, the correlation coefficients R^2 are closer to 1 in the case of the Langmuir equation than the corresponding ones using the Freundlich isotherm at these two pH values. However, predictions are less accurate at the acidic pH value of 3.30 for the Freundlich case. This result can be explained on the basis of poor chain-opening caused by EGDMA, which blocks the access of the copper ions to the adsorption sites.

To explore possible applications of hydrogels as adsorbent materials, a comparison was made of hydrogels synthesized in this work with others that could remove copper ions. Table II shows a quantitative comparison with other acrylic polymeric functionalities. Among the materials shown in the table, hydrogels

Table I. Regressed Parameter Values of Langmuir and Freundlich Isotherms on Hydrogel Sample A1

pH	Langmuir			Freundlich		
	K (L mg^{-1})	q_{\max} (mg g^{-1})	R^2	n	A ($\text{mg}^{1-1/n} \text{L}^{1/n} \text{g}^{-1}$)	R^2
3.30	0.017	104.17	0.4198	3.35	12.73	0.4249
4.20	0.004	263.16	0.9541	3.95	33.00	0.9333
4.70	0.006	294.12	0.9697	2.88	25.13	0.9009

Table II. Comparison of Copper Uptake for Different Materials

Hydrogel	Chelating group(s)	Cu(II) uptake (mg g^{-1})	References
Poly(vinylpyrrolidone/acrylic acid)	—COOH	23	16
Poly(acrylic acid-co-itaconic acid)	—COOH	0.5–99.0	37
Poly[acrylamide/ <i>N</i> -vinyl pyrrolidone/3-(2-hydroxyethyl carbamoyl)acrylic acid]	—COOH, —OH	46	41
Poly(vinylpyrrolidone)/poly(vinylpyrrolidone-co-methylacrylate)	— \bar{N} —, —COOH	35–70 (pH = 2)	27
		75–130 (pH = 5)	
		92–170 (pH = 8)	
Poly(acrylic acid-co-acrylamide)	—COOH, —NH ₂	72.9–211.7	This work

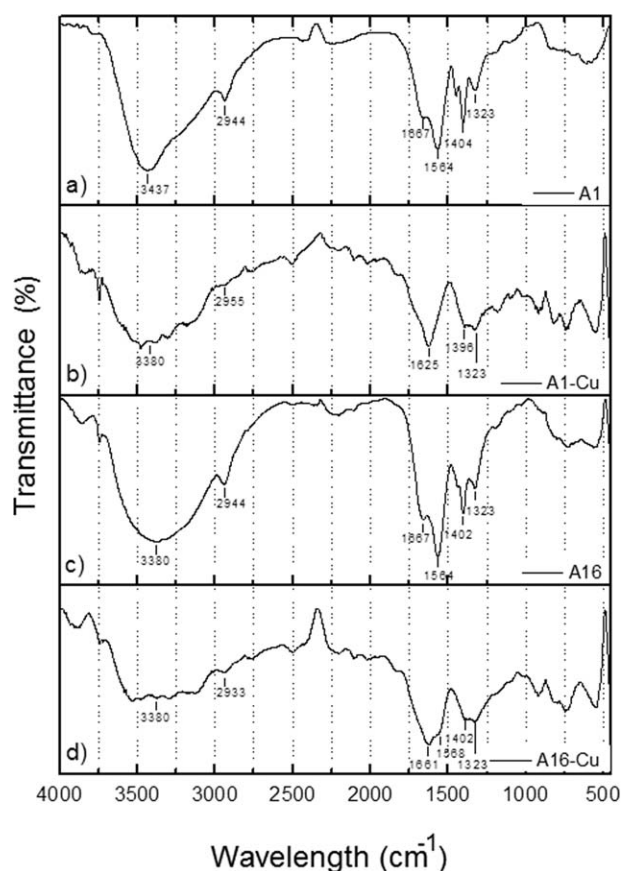


Figure 6. FTIR spectra of hydrogel samples: (a) A1, (b) A1-Cu, (c) A16, and (d) A16-Cu.

with vinylpyrrolidone/acrylic acid are the least efficient in removing copper whereas a hydrogel synthesized by UV photoinitiation shows copper removal capabilities comparable to those of our A1 sample. Our materials have improved copper uptake capacities and show potential to be used in aqueous effluents separations.

FTIR Spectroscopy

Information about the complexation interactions between copper ions and the chelating groups of hydrogels (e.g., $-\text{OH}$ and $-\text{NH}_2$) can be obtained from the FTIR spectra before and after copper uptake. In Figure 6, the FTIR spectra of the fresh hydrogels A1 and A16 [spectra (a) and (c), respectively], as well as with copper adsorbed A1-Cu and A16-Cu [spectra (b) and (d), respectively] are shown. Common characteristics are readily apparent from the spectra. In the case of fresh hydrogels (A1 and A16), bands are observed at 3400 cm^{-1} due to stretching vibrations of the $-\text{OH}$ groups from both the carboxylic acid of the acrylic monomer and from water molecules adsorbed on the surface of hydrogel, as well as the $\text{N}-\text{H}$ bond from acrylamide.^{42–46} Another band is present in the spectra of these two samples at 2942 cm^{-1} due to the stretching vibrations of $\text{C}-\text{H}$ bond related to the hydrocarbon backbone of the polymer (possibly methylene $-\text{CH}_2-$ groups). The presence of these groups is also confirmed by a band at 1450 cm^{-1} attributed to the bending vibration of these moieties.⁴⁶ In the same spectra, two bands are observed in the region between 1500 and 1700

cm^{-1} due to the $\text{C}=\text{O}$ bond: the band at around 1666 cm^{-1} corresponds to the stretching vibrations of carbonyl group from amide group and the band at 1566 cm^{-1} is attributed to carboxylate groups (formed during the neutralization step with KOH in the hydrogel synthesis). Additionally, the $\text{C}-\text{N}$ and $\text{C}-\text{O}$ stretching vibrations from amide and carboxylic moieties are observed in the bands located at around 1400 and 1323 cm^{-1} , respectively.^{8,44–46} When the spectra of the samples A1 and A16 are compared, significant changes are observed in the intensities of bands at 1666 cm^{-1} and 1566 cm^{-1} due to the different percentages of EGDMA used as crosslinking agent as well as to the different monomeric ratios used in the synthesis of these samples. In fact, sample A16 (with the highest amount of EGDMA) shows contributions to these carbonyl bands from the ester part at around 1660 cm^{-1} of this crosslinking agent. On the other hand, the copper uptake by samples A1-Cu and A16-Cu [Figure 6(b,d)] produces changes in some of the band patterns compared to the fresh hydrogels [Figure 6(a,c)]. For example, the band at around 3400 cm^{-1} in both hydrogels appears wider (i.e., less intense and different shape) due to copper influence. This absorption band that appears modified in both samples corresponds to stretching vibrations of hydroxyl groups of the carboxylic acid ($-\text{OH}$) and the $-\text{NH}$ groups of the amide as it was assigned above. The influence of the Cu in the hydrogels is also extended to carbonyl bands (1667 and 1566 cm^{-1}) averaging to a broader band at 1625 and 1661 cm^{-1} in the samples A1-Cu (b) and A16-Cu (d), respectively. In the case of the band at 1625 cm^{-1} (spectrum b), this emerging band could be related to the classical signal known as amide II, whereas the band at 1661 cm^{-1} (spectrum d) due to the presence of the $\text{C}=\text{O}$ from amide seems not to be completely affected by the copper. In contrast, the intensity of the last two bands at 1402 and 1323 cm^{-1} ($\text{C}-\text{N}$ and $\text{C}-\text{O}$, respectively) was clearly affected as a consequence of the Cu ions adsorption.

Results of Elemental Analysis and N_2 Adsorption Measurements

Elemental analysis was conducted on hydrogel samples A1, A16, C1, and C16 to confirm the formation of copolymer through the C/N ratio. The chemical composition of the copolymer was done through the quantification of the nitrogen amount (from acrylamide) that is related to the copolymer network and associated to the total amount of carbon contained in the original monomers and the crosslinking agent.⁴⁷ It can be observed from Table III a decrease in the C/N ratio between samples A and C, corresponding to AA : AM molar ratios of 1.2 : 1.0 and 1.0 : 1.2, respectively. These results confirm that samples from group C contain the highest amount of nitrogen. Moreover, the results obtained for all samples are in agreement with the stoichiometric values used when hydrogels were synthesized. In the case of samples A, the results are also supported from the FTIR results where formation of hydrogels is confirmed. On the other hand, to determine the presence of pores, nitrogen adsorption and desorption measurements were conducted on the synthesized dry (sample A1). The results of these measurements showed a negligible BET surface area of $0.5947 \pm 0.0686\text{ m}^2/\text{g}$ for sample A1 and absence of pores with small dimensions (calculated by the BJH method).^{48,49} These results indicate that

Table III. Elemental Analysis Results on Hydrogel Samples A1, A16, C1, and C16

Sample	%C	%H	%N	%O	C/N
A1	47.32	6.46	4.28	41.94	11.05
A1-T ^a	50.23	5.96	4.91	38.90	
A16	46.64	5.40	6.68	41.12	6.98
A16-T ^a	51.59	6.10	4.26	38.05	
C1	45.72	6.06	11.17	37.05	4.09
C1-T ^a	51.59	6.10	14.63	28.03	
C16	45.37	6.18	11.08	37.37	4.09
C16-T ^a	51.86	6.72	12.74	28.58	

^aT = theoretical value obtained from the stoichiometry of the polymerization reaction.

polymer chains within the dry hydrogels are compacted, impairing the nitrogen molecules to penetrate the internal structure of hydrogel during these measurements.

XPS Analysis

XPS analysis was employed here to study the chemical surface composition of the synthesized hydrogels before and after copper adsorption. The high-resolution of core-level spectra (C 1s, O 1s, N 1s, and Cu 2p) resolved into individual component peaks, are shown in Figure 7 for sample A1. The transition window of C 1s in the case of fresh hydrogel A1 [Figure 7(a)] consists of a strong signal of graphitic carbon at 284.5 eV⁴⁹ which corresponds to the ubiquitous carbon found by the XPS technique mixed with carbon linked to hydrogen atoms.⁵⁰ The shoulder at higher BE is fitted with two signals: one at 286.1 eV which is a typical value for carbon in C—O⁴⁵ or C—N⁵¹ fragments, whereas the signal at 288.0 eV rises when the carbonyl group (C=O) is present.^{49–51} When the hydrogel was contacted with the copper ions solution (sample A1-Cu), the carbon spectrum was fitted with three curve components [Figure 8(a)], similar to the sample before copper adsorption, but in this case the intensity at 288.0 eV increased indicating a higher content of carbonyl carbon. This carbonyl observed by XPS corresponds to the carboxylic group and to the deprotonated carboxylate groups.^{52,53} In the case of the O 1s core level of sample A1 [Figure 7(b)], three components were required to reproduce the spectrum with positions at 532.9, 531.5, and 529.8 eV. The first signal has a typical value for oxygen in carboxylic acids,⁵⁴ and represents the protonated hydroxyl regions of the hydrogel. The second signal is associated to carbonyl oxygen in carboxylic acids⁵⁴ and amides.⁵⁵ The signal at 529.8 eV can be assigned to the amide oxygen, while the spectrum with BE of 531.5 eV would correspond to carbonyl oxygen of the protonated carboxylic groups and the ionized carboxylate form.^{52,53} Furthermore, the analysis of the O 1s spectra of sample A1, shows that the signal intensity at 529.8 eV of carbonyls increased, and achieved an area close to that of the —OH (532.9 eV) when this sample was treated with the copper sulfate solution [Figure 8(b)]. This fact suggests a protonation of the carboxylate moieties likely due to acidification during the copper retention experiments, even though, there are remaining carboxylate groups (detected

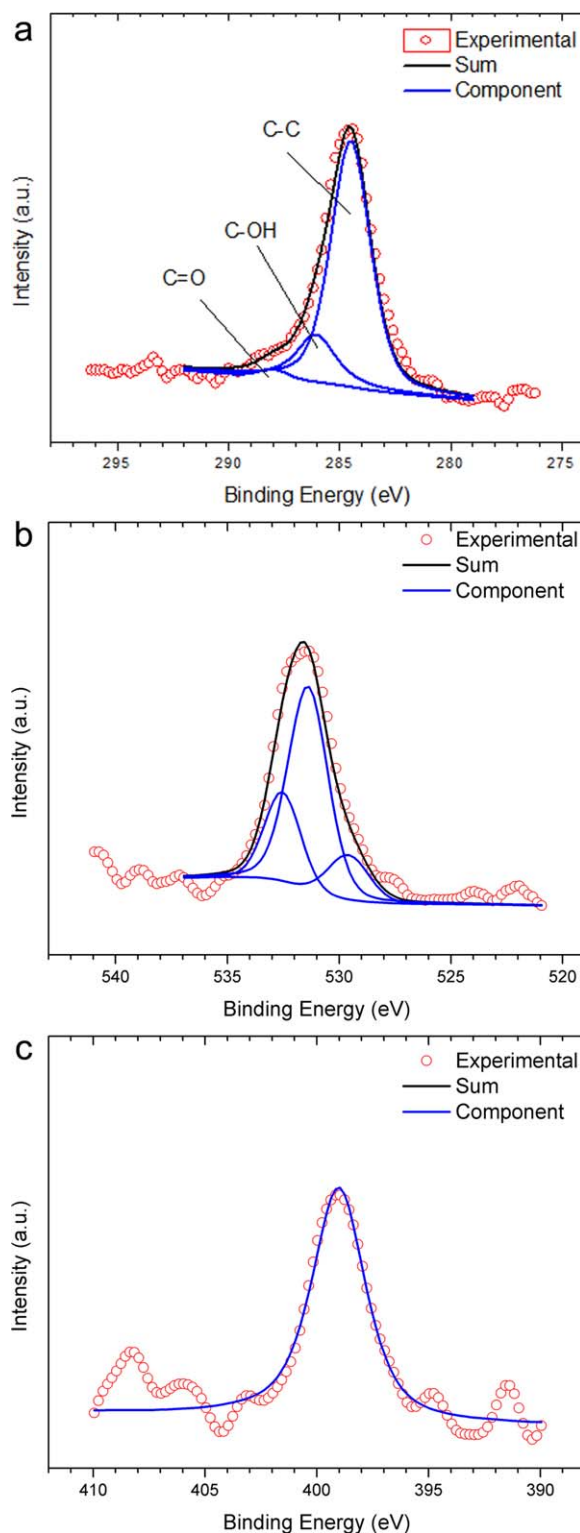


Figure 7. XPS high-resolution spectra collected for sample A1. a) C 1s, b) O 1s, c) N 1s. [Color figure can be viewed in the online issue, which is available at wileyonlinelibrary.com.]

by FTIR) available for copper retention. The spectrum for N 1s was fitted with only one curve whose binding energy (BE) matches with the energy found in nitrogen atoms from amide groups^{51,54} in the case of sample A1 [Figure 7(c)] and remained

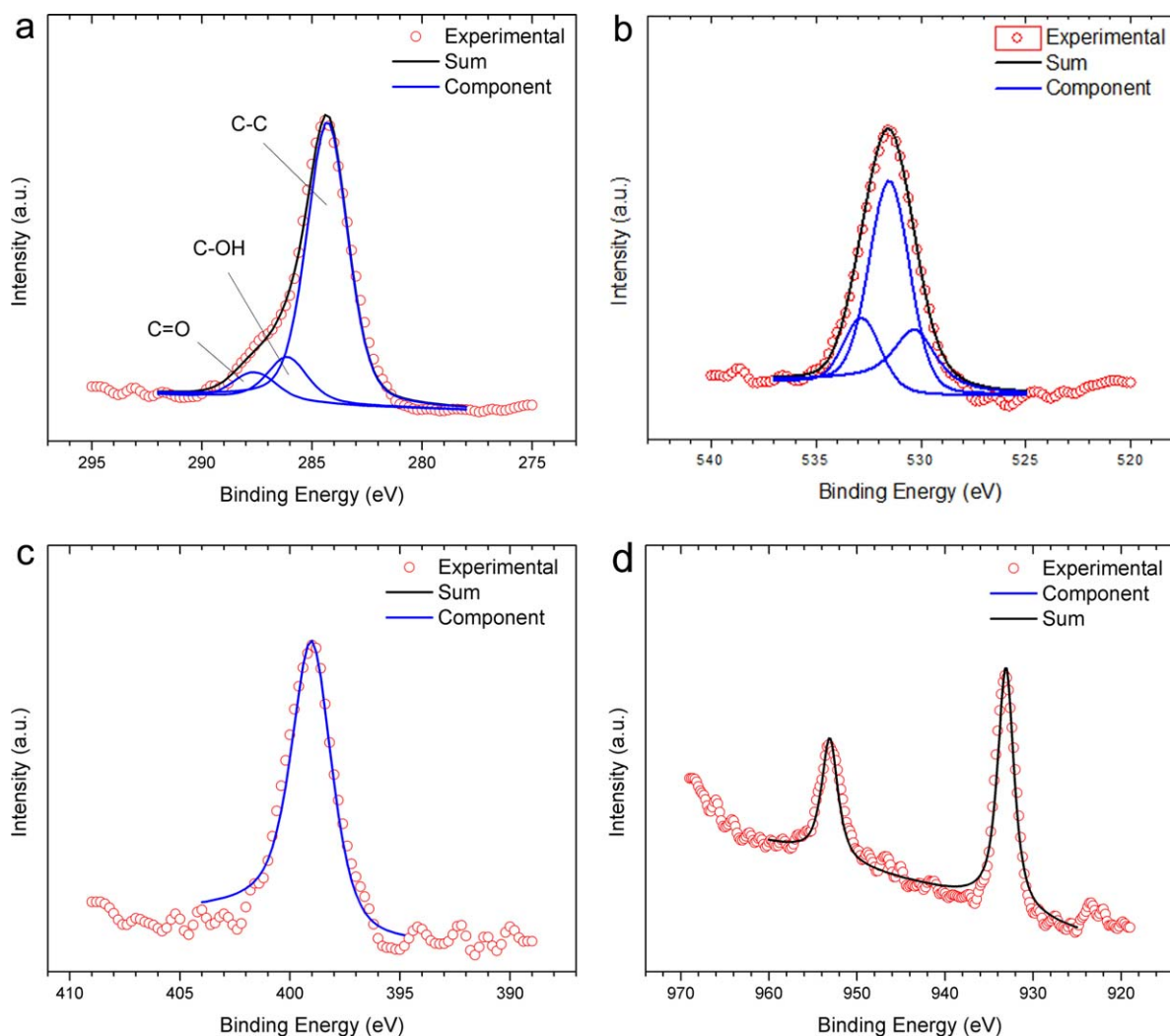


Figure 8. XPS high-resolution spectra collected for sample A1-Cu. a) C 1s, b) O 1s, c) N 1s, d) Cu 2p. [Color figure can be viewed in the online issue, which is available at wileyonlinelibrary.com.]

almost invariant in sample A1-Cu [Figure 8(c)]. These results suggest that copper did not affect the chemical environment of the amide group; however, the nitrogen center has a pair of electrons and then a negative partial charge that could be stabilized by copper (II) cations. The Cu 2p spectra of sample A1-Cu [Figure 8(d)] shows the presence of copper, whose split spectrum from the $2p_{3/2}$ and $2p_{1/2}$ core level was fitted with only one curve. The position of the $2p_{3/2}$ signal at 933 eV indicates the divalent character of the copper cation,⁵⁶ which is likely coordinated to the carboxylate groups since this deprotonated form predominates over the carboxylic groups. In addition to XPS information, the FTIR spectroscopy suggested that the carboxylate groups coordinated the copper cations through one oxygen via a monodentate coordination.⁴⁶

CONCLUSIONS

Hydrogels were synthesized employing acrylic (AA and AM) monomers and applied in the removal of copper ions from

aqueous solutions. Hydrogel samples from group A (with high content of acrylic acid) showed the maximum swelling capacity (27,500%). This swelling degree is advantageous for copper uptake due to a higher exposure of pendant functional groups. Completed polymerization reaction and the absence of residual monomers were demonstrated by $^1\text{H-NMR}$ which is a desirable feature if the hydrogels are to be used for industrial applications. The use of redox initiators in the synthesis route demonstrated a significant improvement in polymerization times compared to the ones when photocatalysts were used. These results make the synthesis route used in this work more attractive to prepare polymeric hydrogels due to an ease of implementation and the use of room conditions. Short copper uptake times of 20 min were obtained from kinetic measurements and a maximum of 2 h of contact time reflecting the presence of minimal mass-transfer resistances. Results showed equilibrium adsorption capacities higher than the corresponding of other materials found in the literature. Complexation interactions between copper ions and the chelating groups of hydrogels and

the presence of a monodentate copper-carboxylate moiety of synthesized hydrogels were determined based on the FTIR and XPS results. A simple synthesis route for the preparation of hydrogels with high copper uptakes and enhanced physical properties were demonstrated in this work.

ACKNOWLEDGMENTS

The authors thank CONACyT for the scholarship of Moran-Quiroz and Dr. Gustavo Rangel-Porras for his support in the BET analysis. They also thank University of Guadalajara for financial support.

REFERENCES

1. Jiménez, B. E. In *Environmental Pollution in Mexico: Causes, Effects and Appropriate Technology* (In Spanish: *La Contaminación Ambiental en México: Causas, Efectos y Tecnología Apropiada*). Limusa Ed., México, **2001**; p 926.
2. Sharma, R. K.; Agrawai, M.; Marshall, F. *Ecotox. Environ. Safe.* **2007**, *66*, 258.
3. Mireles, A.; Solís, C.; Andrade, E.; Lagunas-Solar, M., Piña, C.; Flocchini, R. G. *Nucl. Instrum. Meth. B* **2004**, 219–220, 187.
4. World Health Organization (WHO). *Guidelines for Drinking-Water Quality: Incorporating First Addendum*. Vol. 1, Recommendations, 3rd ed. World Health Organization: Geneva, 2008.
5. USEPA. *Quality Criteria for Water*, **1986**. Available at: <http://water.epa.gov/scitech/swguidance/standards/criteria/current/index.cfm>. Accessed April, 2013.
6. Diario Oficial de la Federación, Official Mexican Regulation Project PROY-NOM-250-SSA1–2007 Environmental Health. Water for human consumption. Allowable limits of water quality, surveillance, and quality control assessment of supply systems. [In Spanish: Proyecto de Norma Oficial Mexicana, PROY-NOM-250-SSA1–2007, Salud Ambiental. Agua para uso y consumo humano. Límites permisibles de calidad del agua, vigilancia y evaluación del control de calidad de los sistemas de abastecimiento]. Mexico, City, Mexico. Available at: www.dof.gob.mx/. Accessed March, 2013.
7. USEPA. *Environmental Health Criteria Monographs from IPCS INCHEM*, Available at: <http://www.inchem.org/pages/ehc.html>, accessed December 2011.
8. Pratih, V. D.; Patel, M. P.; Patel, R. G. *J. Macromol. Sci. A* **2007**, *44*, 769.
9. Bessbousse, H.; Rhlalou, T.; Verchère, J. E.; Lebrun, L. *J. Membr. Sci.* **2007**, *307*, 249.
10. Oliva, J.; de Pablo, J.; Cortina, J. L.; Cama, J.; Ayora, C. *J. Hazard. Mater.* **2011**, *194*, 312.
11. Chaudhari, L. B.; Murthy, Z. V. P. *J. Hazard. Mater.* **2010**, *180*, 309.
12. Hongbo, L.; Jing, L.; Zhanjun, Y.; Qin, X.; Chuantao, H.; Jinyun, P.; Xiaoya, H. *J. Hazard. Mater.* **2011**, *191*, 26.
13. Asthana, A.; Falcoz, Q.; Sessiecq, P.; Patisson, F. *Ind. Eng. Chem. Res.* **2010**, *49*, 7605.
14. Shawky, H. A.; Ali El-Hag, A.; El-Sheikh, R. A. *J. Appl. Polym. Sci.* **2006**, *99*, 2904.
15. Bajpai, S. K.; Johnson, S. *J. Macromol. Sci. A* **2007**, *44*, 285.
16. El-Hag Ali, A.; Shawky, H. A.; Abd El Rehim, H. A.; Hegazy, E. A. *Eur. Polym. J.* **2003**, *39*, 2337.
17. Lee, E.; Strangio, W.; Lim, B. In: *Proceedings of the 41st Industrial Waste Conference*; Bell JH, Ed. Lewis Publishers, Inc.: Chelsea, MI, **1986**; Purdue University, pp 652–658.
18. Lee, C. K.; Tavlarides, L. L. *Metal. Trans. B* **1983**, *14B*, 153.
19. Chang, L. Y.; McCoy, B. J. *Environ. Prog.* **1991**, *10*, 110.
20. Eckenfelder, W. W.; Patoczka, J.; Watkin, A. T. *Chem. Eng.* **1985**, *92*, 60.
21. Tchobanoglous, G. *Wastewater Engineering: Treatment/Disposal/Reuse*, 4th ed.; Metcalf and Eddy, Inc., McGraw Hill Book Company: New York, NY, **2004**; p 1819.
22. Orozco-Guareño, E.; Santiago-Gutierrez, F.; Morán-Quiroz, J. L.; Hernández-Olmos, S. L.; Soto, V.; de la Cruz, W.; Manriquez, R.; Gómez-Salazar, S. *J. Colloid. Interf. Sci.* **2010**, *349*, 583.
23. Katime, I.; Rodríguez, E. *J. Macromol. Sci. A* **2001**, *38*, 543.
24. Şolpan, D.; Güven, O. *J. Macromol. Sci. A* **2005**, *42*, 485.
25. Yian, Z.; Ai Qin, W. *J. Hazard. Mater.* **2009**, *171*, 671.
26. Abdel-Halim, E. S.; Al-Deyab, S. S. *Carbohydr. Polym.* **2001**, *86*, 1306.
27. Yildiz, U.; Ferkan Kemik, Ó.; Hazer, B. *J. Hazard. Mater.* **2010**, *183*, 521.
28. Xiao-Jie, J.; Shi-Bo, Z.; Ming-Yu, Z.; Rui, X.; Lihua, Y.; Liang, C. *J. Hazard. Mater.* **2009**, *167*, 114.
29. Hyun Jang, S.; Gyu Jeong, Y.; Gil Min, B.; Seok Lyoo, W.; Cheol Lee, S. *J. Hazard. Mater.* **2008**, *159*, 294.
30. Odian, G. In *Principles of Polymerization*, 3rd ed. Wiley-Interscience: New York, **1991**; Chapter 3, pp 199–334.
31. Sarac, A. S. *Prog. Polym. Sci.* **1999**, *24*, 1149.
32. Yagci, C.; Yildiz, U. *Eur. Polym. J.* **2005**, *41*, 177.
33. Orozco-Guareño, E.; Campos Almaraz, A. N.; Reyes, G. I.; López-Ureta, L. C.; Gonzalez Alvarez, A. *J. Therm. Anal. Calorim.* **2006**, *86*, 511.
34. Crites, R.; Tchobanoglous, G.; Camargo, M.; Pardo, L.; Mejia, G.; *Water Treatment in Small Populations* [In Spanish: *Tratamiento de Aguas en Pequeñas Poblaciones*]; McGraw-Hill: Bogota, Colombia, 2000, p 776.
35. Sreesai, S.; Sthiannopkao, S. *Can. J. Civil Eng.* **2009**, *36*, 709.
36. Grabowska, B.; Holtzer, M. *Arch. Metall. Mater.* **2009**, *54*, 427.
37. Rodriguez, E. Katime, I. *J. Appl. Polym. Sci.* **2003**, *90*, 530.
38. Schott, H. *J. Pharm. Sci.* **1992**, *81*, 467.
39. Tang, Q. W.; Wu, J. H.; Lin, J. M.; Sun, H.; Ao, H. Y. *e-Polymers* **2008** Feb 6;article: 21.
40. Karadag, E.; Uzum, O. B.; Saraydin, D. *Eur. Polym. J.* **2002**, *38*, 2133.

41. Dadhaniya, P. V.; Patel, M. P.; Patel, R. G. *J. Macromol. Sci. A* **2007**, *44*, 769.
42. Tang, Q. W.; Lin, J. M.; Wu, J. H. *React. Funct. Polym.* **2007**, *67*, 489.
43. Lu, T.; Shan, G. R.; Shang, S. M. *J. Appl. Polym. Sci.* **2010**, *118*, 2572.
44. Silverstein, R. M.; Webster, F. X.; Kiemle, D. J. In *Spectroscopic Identification of Organic Compounds*, 7th ed. Wiley: USA, **2005**.
45. Mahdavinia, G. R.; Pourjavadi, A.; Zohuriaan-Mehr, M. J. *J. Appl. Polym. Sci.* **2006**, *99*, 1615.
46. Nakamoto, K. *Infrared and Raman Spectra of Inorganic and Coordination Compounds: Applications in Coordination, Organometallic, and Bioinorganic Chemistry. Part 2: Infrared and Raman Spectra of Inorganic and Coordination Compounds*, 6th ed. Wiley: New Jersey, **2009**; p 424.
47. Ju, X. J.; Chu, L. Y.; Liu, L.; Mi, P.; Lee, Y. M. *J. Phys. Chem.* **2008**, *112*, 1112.
48. Barret, E. P.; Joyner, L. G.; Halenda, P. P. *J. Am. Chem. Soc.* **1951**, *73*, 373.
49. Wang, C.; Jin, Q.; Wang, Y.; Yin, H.; Xie, H.; Cheng, R. *Mater. Lett.* **2012**, *68*, 280.
50. Setsuhara, Y.; Cho, K.; Shiratani, M.; Sekine, M.; Hori, M.; Ikenaga, E. *Thin Solid Films* **2010**, *518*, 3555.
51. Xu, F. J.; Zheng, Y. Q.; Zhen, W. J.; Yang, W. T. *Colloid Surf. B* **2011**, *85*, 40.
52. Mitra, S. B.; Lee, C. Y.; Bui, H. T.; Tantbirojn, D.; Rusin, R. *P. Dent. Mater.* **2009**, *25*, 459.
53. Higo, M.; Miake, T.; Mitsushio, M.; Yoshidome, T.; Ozono, Y. *Appl. Surf. Sci.* **2008**, *254*, 3829.
54. National Institute of Standards and Technology. (NIST), NIST X-Ray Photoelectron Spectroscopy Database, (n.d.). Available at: <http://srdata.nist.gov/xps/>, accessed May 2012.
55. Lai, L.-J.; Yang, Y.-W.; Lin, Y.-K.; Huang, L.-L.; Hsieh, Y.-H. *Colloid Surf. B* **2009**, *68*, 130.
56. Wagner, C. D.; Riggs, W. M.; Davis, L. E.; Moulder, J. F.; Muilenberg, G. E. *Handbook of X-Ray Photoelectron Spectroscopy*; Perkin-Elmer Corporation: Minnesota, **1979**.